DOI: 10.1002/adma.200602042

Supramolecular Structure of Extrinsically Chiral Porphyrin Hetero-Assemblies and Achiral Analogues**

By *Roberto Matassa*, *Marilena Carbone*, *Rosaria Lauceri*, *Roberto Purrello*, and *Ruggero Caminiti**

Nature uses chiral information to achieve the excellent degree of selection and efficiency peculiar to all living systems. But chirality is also receiving growing interest for the possible technological applications that span from chiroptical devices[1] to asymmetric catalysis,[2] memory systems,[3,4] and others.[5] The transfer of chiral information to achiral molecules through non-covalent interactions, expressed at a supramolecular level, has, in particular, gained great consideration.[6,7] In fact, non-covalent synthesis, especially when molecular recognition and self-assembly processes are involved,[8] presents many advantages: i) it is not time consuming, ii) it does not lead to side products, and iii) it dose not require an external energy source for reaction.

When a chiral structure is imprinted onto an assembly of symmetric molecules by a chiral template or by macroscopic forces (i.e. mechanical effects),[9,10] through mere non-covalent interactions, the resulting supramolecular chiral system may experience two different fates following the template chiral structure modification or removal: i) if the species is under thermodynamic control, it loses the imprinted chiral properties but, ii) if the species is kinetically inert, then it can preserve the imprinted chiral properties for hours, months or even longer. The last case is defined as "memory" effect.[11–13] The chiral memory phenomenon is of particular interest because, used in combination with the non-covalent strategy, permits to assembly supramolecular species able to perform predetermined functions coupled with chiral discrimination.[14,15] With these premises, it is clear that understanding the forces involved and the mechanism accompanying induction, modulation and memory of supramolecular chirality could allow for the rational design and assembly of chiral supramolecular systems. Taking advantage of the chiral memory approach, we have recently published the non-covalent synthesis of chiral porphyrin hetero-aggregates, templated by polypeptides or aminoacids.[16–18] These aggregates keep memory of the imprinted chirality that is maintained, even after removing the chiral template. Furthermore, their interactions in the absence of chiral templates leads to achiral species.

Here, we present the first structural determination of a porphyrin (chiral) hetero-aggregate through energy dispersive X-ray diffraction analysis (EDXD) because of the poor crystalline character of the aggregates. The achiral components are represented by meso-tetrakis(N-Methylpyridium-4-yl)porphinato-copper(II) (CuT4-cationic) and meso-tetrakis-(4-sulfonatophenyl)porphyrin (H_2TTPS-anionic), while L-phenilalanine is used as chiral mould. Also, a comparison is reported with the amorphous hetero-aggregate structure that the same porphyrins form in the absence of the chiral template. The aggregation process may involve one type of porphyrin only, the homo-assemblies or homo-aggregates,[19,20] or more porphyrins of different type,[21–23] the hetero-assemblies of hetero-aggregates, for instance cationic-anionic hetero-assemblies. Morphology and structure of the porphyrin aggregates are responsible for the porphyrin physical and chemical physical properties. In fact, chiral properties are bi-univocally related to the 'assemblies' structure. However, circular dichroism (CD) was, so far, the only chiral diagnostic tool for hetero aggregates. Our structural study of L-Phe-imprinted hetero-aggregates of CuT_4-H_2TTPS compared to the equivalent non-imprinted sample in solid state has evidenced that the template imprints an α-helix superstructure responsible for the CD properties. The lack of template during the aggregation leads to a randomly arranged structure and a lack of CD signal in the region of absorbance of the porphyrins.[24–26]

The experimental structure functions (SF) qI(q)M(q) collected in the reciprocal space in the range 0 to 17 $Å^{-1}$ show the typical damped oscillations of amorphous samples (Fig. 1A). However, the functions of the two samples exhibit marked differences. The intensity of the first two peaks is 3 times lower for the non-imprinted than for the imprinted samples, an indication of a more disordered molecular packing. Furthermore, a slight peaks shift characterizes the SFs of

[*] Prof. R. Caminiti, Dr. R. Matassa
Dipartimento di Chimica
Università degli Studi di Roma "La Sapienza"
P. le A. Moro 5, 00185 Roma (Italy)
E-mail: r.caminiti@caspur.it
Dr. M. Carbone
Dipartimento di Scienze e Tecnologie Chimiche
Università di Torvergata
Via della Ricerca Scientifica 1, 00133 Roma (Italy)
Dr. R. Lauceri
IBB, CNR-Sezione di Catania
Dipartimento di Scienze Chimiche
Viale A. Doria 6, 95125 Catania (Italy)
Prof. R. Purrello
Dipartimento di Scienze Chimiche
Università di Catania
Viale A. Doria 6, 95125 Catania (Italy)

[**] The authors would like to thank Ateneo 2006 for their financial support of this research. Supporting Information is available online from Wiley InterScience or from the author.

ADVANCED MATERIALS

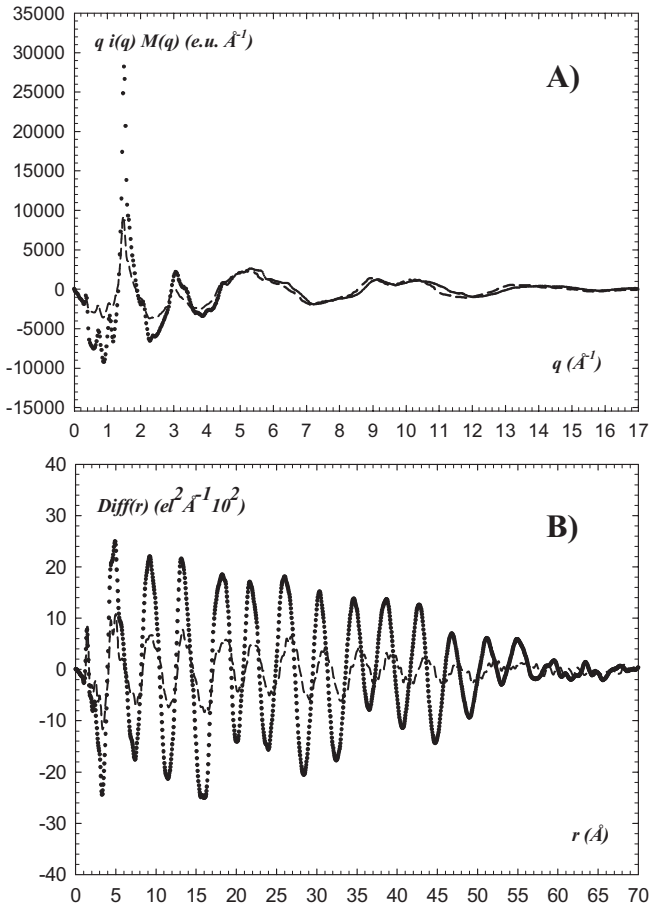

Figure 1. Experimental X-ray diffraction patterns of the investigated samples: A) Experimental SF of the imprinted (black dots) and of non-imprinted aggregates (red dots). B) Experimental Diff(r)s of imprinted (black dots) and of non-imprinted aggregates (short dash).

the two samples more marked in the region of the intramolecular interactions (from ~5 to 17 $Å^{-1}$).

The imprinted sample's SF shows a main broad peak at 1.50 $Å^{-1}$ followed by less intense shoulders at 1.65, 2.07 $Å^{-1}$ and by a second-order peak of the main one at 3.05 $Å^{-1}$. This satellite peak in porphyrin assemblies is associated to H-type aggregation belonging to a cofacial configuration where the molecules form a vertical stack. The peak positions are closely related to intermolecular distance, as reported by R. Caminiti et al.[27] The remaining experimental structure function shows one broad peak at ~ 5.30 $Å^{-1}$ and two large oscillations, related to intramolecular interactions. The non-imprinted sample's SF exhibits a main broad peak at 1.47 $Å^{-1}$, a less intense shoulder at 2.03 $Å^{-1}$ and a second-order peak at 3.02 $Å^{-1}$. The Fourier transform of the structure functions yields the radial distribution function Diff(r) from 1 to 70 Å that provides direct information on the aggregation state. The difference of the two samples is even more marked here (Fig. 1b). The imprinted sample shows a structural range from 1 to ~60 Å with peaks of decreasing intensity. The non-imprinted sample has similar trend of peaks, but in a shorter range, i.e. from 1 to ~47 Å and of much lower intensity, related to the more disordered structure. The first two peaks at ~1.45 Å and ~2.45 Å are attributed to intramolecular interactions; the peaks from ~4.90 Å to ~13.50 Å are due to both intramolecular and intermolecular interactions. All following peaks are due to the intermolecular interactions only.

In order to solve the structure we needed to combine information gathered from the previous structural studies of porphyrins with that extracted from experimental diffraction patterns.

Although some porphyrins possess an extended aromatic system the structure is highly flexible, and several ways of inducing nonplanar deformations of the macrocycle are known.[28–30]

The main non-planar deformations are the ruffling, a twisting around the M–N_p bond, such as in CuTPP and PdTPP,[31] the saddling, i.e the displacement of the pyrrole rings alternately above and below the mean porphyrin plane, for example in CuT4,[32] the doming often observed in five-coordinate complexes, due to the axial ligand such as in MImCoTPP,[33] and the waving, where one pair of opposing pyrrole rings is displaced up and down, while the other pair is twisted in the same direction along their M–N_p bond, such as in NiTMeP.[34]

Several parameters influence the porphyrin assembling. The key effect is the intermolecular interaction of the extended aromatic systems. But the type of metal, the peripheral substituents and the molecular packing in solid state also play a role. The incorporation of the metal atoms of different sizes in the center of the macrocycle[35] as well as porphyrins peripheral substitutions influence the non-planar distortion.[33,36] It is worth noticing that packing forces also act to modify the degree of molecular deformation and/or impose distortions of other symmetries upon the macrocycle in the solid state.

The starting setup for structural analysis of the template-imprinted sample were available data (experimental CuT_4 and theoretical H_2TTPS) on corresponding homo-aggregates.[31,32,37,38] No data are available, in fact, for hetero-aggregates. The theoretical structural analysis has shown that an increasing molecular tilting decreases the intensity of the main peak. To recover the theoretical peak intensity, further dimers were added in stacking configuration. Molecular distortions and rotation of the substituents have opposite effects on the main peak and the shoulders. The variations of the dihedral angle α (see the structural building in Fig. 2) causes a decrease of the main peak and an increase of the shoulder at 1.65 $Å^{-1}$. An increase of the dihedral angle α also suppresses the intensity of the peak at 1.50 $Å^{-1}$ and increases the intensity of the shoulder 2.07 $Å^{-1}$. Molecular rotations around the stack axis below 20° increase the main peak and decrease both shoulders (Fig. 1S of the Supporting Information). At 20° the shoulders are completely suppressed and beyond this rotation value the main peak decreased and a spurious peak at 1.07 $Å^{-1}$ appears (Fig. 2S of the Supporting Information).

Molecular slipping affects the main peak position. Tests were made by shifting the dimers with respect to each other along the x, y or z-axis A slipping along the x or y-axis causes

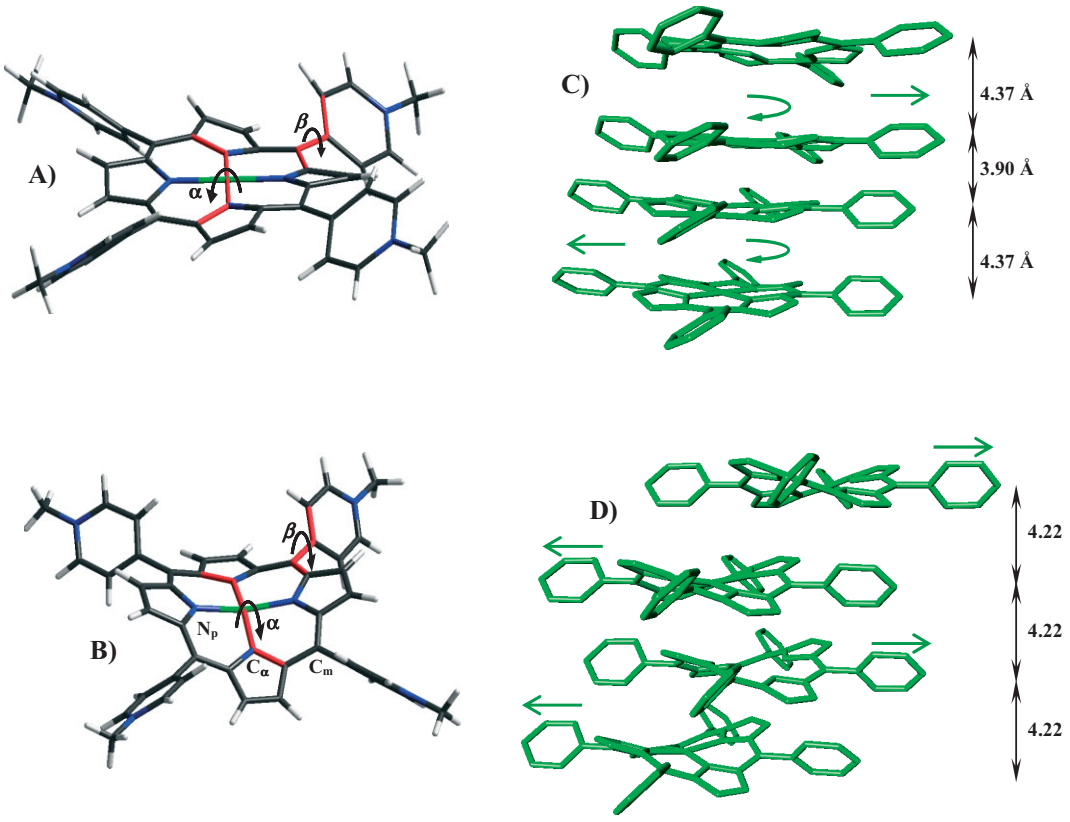

Figure 2. Structural model building of the template-imprinted anb the non-imprinted sample. A) Basic molecular structure of the saddling distortion of meso-substituted porphyrin; Np, Cm, Cα, α and β represent the pyrrole ring p-nitrogen atom, meso-substituents m-carbon atom, pyrrole ring α-carbon atom, α dihedral angle formed by two nitrogens atom in opposite pyrrole rings (CαNp●●●●NpCα) and β dihedral angle between the mean plane of the porphyrin skeleton and the planes of the meso-substituents. B) Shows ruffling distortion of the porphyrin core. C) 3D view of two dimers of the template imprinted sample. D) 3D view of four monomers of the non-imprinted sample.

a shift of the main peak towards low values of q(Å^{-1}). A slipping in the xy plane produces a broadening of the main peak as well as an asymmetric tail on the low q(Å^{-1}) values side and a decrease of the intensity. The shift related to the slipping along the z-axis depends strongly on the interplanar distances, whether they are increased or reduced.

By synchronizing all structural parameters we determined the structure of the template-imprinted sample. The experimental and theoretical SFs and Diff(r)s are reported in Figure 3A and B. To simplify the model description, the structural parameters are referred to the centres of mass of the single molecules.

The best agreement was obtained when the following parameters were used: for the cationic porphyrin, i) a ruffling distortion shape, ii) a displacement of the dihedral angle α of the pyrrolic rings of (11°±1°), iii) a clockwise rotation of the four meso-substituents to give a dihedral angle β of (35°±4°) (Fig 2B). The porphyrin plane of the anionic molecule is less distorted. The dihedral angle α is (6°±1°) and the peripheral substituent show a clockwise rotation of the substituents to give a dihedral angle β of (40°±4°) °(Fig. 2C). The atomic cartesian coordinates corresponding to this dimeric model are available in the Supporting Information Table 1S.

Most important, the best fit process brought a molecular arrangement of eight dimers in stacking configuration, forming a helix. A model of the template imprinted sample is presented in Figure 4A.

The molecules of one dimer are separated by (4.37±0.10) Å and rotated of 5°. The shift of the molecules with respect to each other in the xy plane is (0.05±0.01) Å along the x and of (0.51±0.01) Å along the y-direction. The dimer units are rotated around the stack axis of (20°±2°) and separated by an interplanar distance of (3.90±0.10) Å. The slipping along the x and y-axis displace the dimers in deformed helical arrangement, forming approximately one half of a complete turn around the helix axis, characterized, on average, by a radius of (5.50±0.30) Å and by a pitch length of (62.17±0.20) Å. A system of polar coordinates of the porphyrins centers of mass is shown in Figure 4C and the corresponding numerical values are reported in table 2S. Further theoretical models in terms of different dimers and of non dimeric hetero-aggregates are available in figure 1S-4S as Supporting Information.

From the above description we can conclude that: i) The template imprints the chiral structure to the CuT4- H_2TTPS cationic-anionic hetero-assembly.

ADVANCED MATERIALS

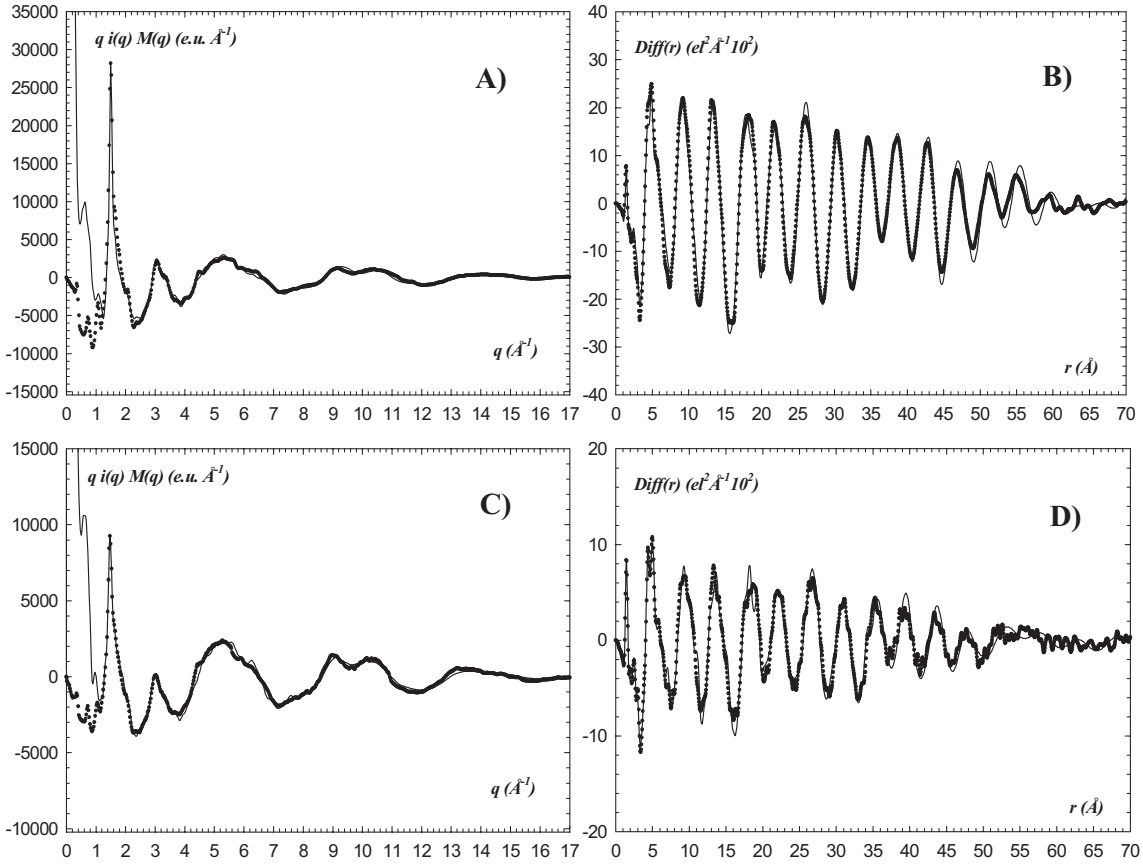

Figure 3. Structural analyses of the hetero-porphyrins. A) Experimental structural SF (black dots) and theoretical curve (black solid line) calculated for 8 dimers of the imprinted CuT4-H2TPPS hetero-aggregate and, B) the corresponding Diff(r). C) Experimental SF (red dots) and theoretical curve (black solid line) calculated for 16 molecules of the non-imprinted CuT4-H2TTPS hetero-aggregates and, D) the corresponding Diff(r)-form.

ii) The non-imprinted sample shows different SF and Diff(r) compared to the chiral one. Optimization of the molecular distortions leads to a saddling shape for both the CuT4 and the H_2TTPS molecules. Furthermore, CuT4 and H_2TTPS are characterized by a pyrrolic dihedral angles of (12°±1°) and (9°±1°), respectively. To match the intensity of the main peaks, the model required an increasing and an alternating of the dihedral angle β of (56°±4°) and (60°± 4°) for the peripheral substituents of the CuT4 and H_2TTPS, respectively. In order to show the porphyrin aggregation, the centers of mass of molecules are plotted in Figure 4B and their values are reported in Table 2S.

iii) The arrangement of the non template imprinted sample is disordered.

iv) The porphyrins are not rotated and they are separated by a average interplanar distance of (4.22 ± 0.21) Å (Fig. 2D). Furthermore, the porphyrins show a constant slipping along the y-axis of 0.87 Å and a series of series of short sharp turns of the molecules, in a zig-zag shape along the y-axis (Fig. 4D).

It is worth noting that the suprachiral structure is strictly related to the use of a single isomer of the template imprinting agent. A use of a template racemic mixture yields porphyrin hetero-aggregates without associated circular dichroism, hence achiral.

Once established the molecular structural stacking of both chiral and achiral samples a further test was made in order to check whether the structure extends in the *xy* plane. Similar columns of molecules were added in order to build up a 3D structure. Several shifts and rotation of the stacks were tested, but no significant improvement of the theoretical structural function was found.[39] The final fitting procedure yielded a good agreement between the experimental data and theoretical peaks (Fig. 3) with a R_{Hamilton} estimate error of 18.64 % for the chiral 15.64 % for the achiral sample respectively.

We prepared two porphyrin cationic (CuT4) and anionic (H_2TTPS) hetero-assemblies, one of which was templated with L-Phe. The structural analysis of the two samples by EDXD technique shows that the chiral template imprints a suprachiral structure to the porphyrin aggregate. In the suprachiral aggregate the cationic and anionic porphyrins exhibit a ruffling distortion and form a dimeric arrangement in an α-helix shape, separated by two different interplanar distances.

The preparation of the aggregates without inclusion of the template yields an amorphous molecular arrangement, hence an achiral structure. Both macrocycles of the hetero-aggre-

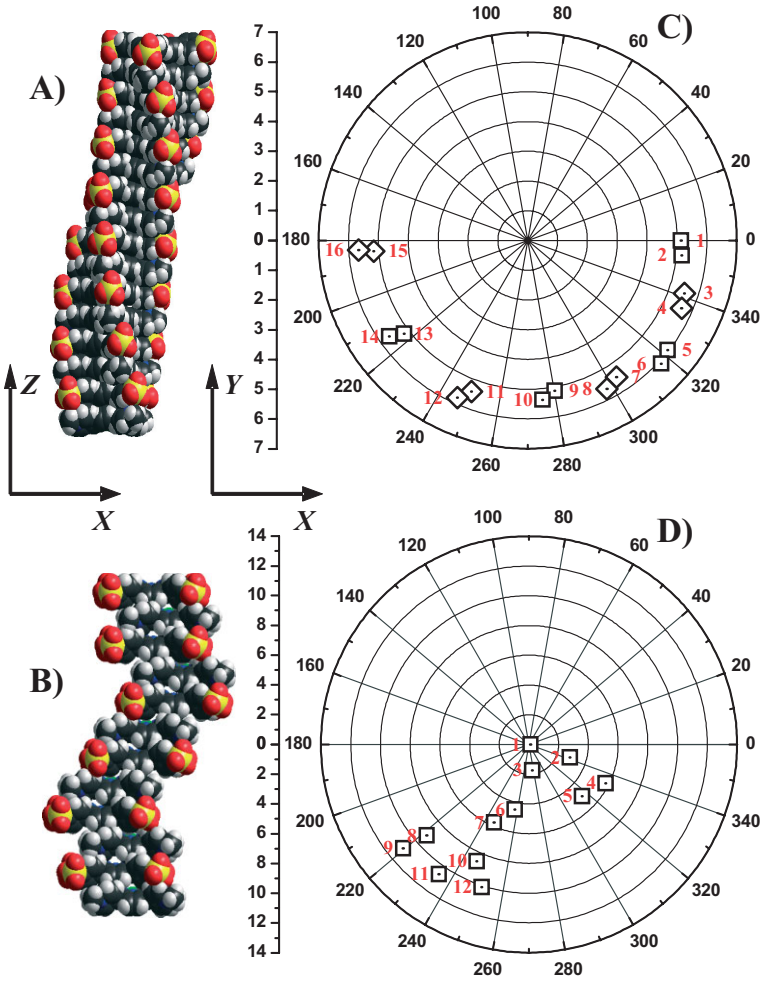

Figure 4. 3D molecular packing of the chiral and the achiral samples: A) 3D view of the chiral imprinted sample. B) 3D view of the achiral non-imprinted sample. Polar plots of the centers of mass viewed from the stack-axis: The stacking axis is perpendicular to the graphic plane and the label numbers increase along the z-axis from 1 to N. The initial ray of the polar coordinate system coincides with the positive x-axis, and that the ray of 90° coincides with the positive y-axis. C) The imprinted sample shows a dimeric helix aggregation forming approximately one half of a complete turn around the helix axis. D) The non-imprinted sample shows a disordered molecular packing, characterized by two clusters of six stack molecules each 180° rotated around the stack axis.

gates are characterized by a pronounced distortion of the saddling type. The different molecular distortions can be attributed to packing effects in the solid state. The porphyrins in the achiral sample are arranged in a stacking configuration marked by a slipping disorder forming a zig-zag shape, stacked by regular interplanar distance.

Experimental

Sample Preparation: Equimolar amount of each porphyrin (the addition order of the two porphyrins has no relevance) were added to a 200 mL aqueous solution of D- or L-Phe 8×10^{-3} M (extra-pure Milli-Q water was used throughout the procedure). Each addition resulted in a porphyrin concentration of 4 μM. After three couples of additions of the cationic and the anionic porphyrin (the final concentration in solution of each porphyrin is equal to 12 μM). The aminoacid was removed from the solution by mean of various centrifugation steps, using Centricon filters (cut-off = 10 KDa). The concentration of phenylalanine was checked both in the aggregate solution and in the filtrate by fluorescence (λ_{ex} = 218 nm, λ_{em} = 284 nm). Here is worth noting that the lowest detectable concentration of Phe is of order of 0.01 μM, while the minimum Phe concentration necessary to induce a chiral structure in the porphyrin hetero-aggregate is of the order of 100 μM [16]. Three further "cleaning" centrifugation steps were performed even after no Phe was detected in the sample. After the amino acid removal, the aggregates were suspended again in 200 mL aqueous solution and various equimolar addition of CuT4 and H_2TTPS were performed until the desired amount of aggregate was assembled (in particular, three couples of additions of 4 μM in each porphyrin were still done, while all the following additions were of the order of 10 μM). When all the necessary growing steps were performed, the aggregate solution was maintained to 45–50 °C until complete water evaporation. The same procedure were followed for the assembly of the CuT4-H_2TTPS chiral hetero-aggregate in the presence of D-Phe and, then, for the aminoacid removal (Fig. 5S) [40].

Finally, the CuT4-H_2TTPS achiral hetero-aggregate was prepared according with the following procedure. Equimolar amounts of each porphyrin (the addition order of the two porphyrins has no relevance) were added to a 200 mL aqueous solution (extra-pure Milli-Q water was used throughout the procedure) until the desired amount of aggregate was assembled. In particular, six couples of additions of 4 μM in each porphyrin were first done, while all the following additions were of the order of 10 μM in each porphyrin. When all the necessary growing steps were performed, the aggregate solution was maintained to 45-50 °C until complete water evaporation. The powder samples were, then, recovered for EDXD characterization.

EDXD Data Collection and Processing: The characterization of compounds was carried out by energy dispersive X-ray diffraction technique [41,42]. The very finely pulverized sample was compressed into pellets. Data were recorded with a custom built X-ray energy scanning diffractometer [43], consisting of a Seifert X-ray HV generator supplying a water-cooled tungsten X-ray source, with maximum power of 3.0 kW. The bremsstrahlung (braking radiation) of the X-ray source was used. Operating conditions were: high voltage supplies 40 kV, current intensity 50 mA. A germanium solid-state detector (SSD) was used for recording the diffraction spectra. The SSD was linked to a multichannel analyzer by an electronic chain. A set of collimating slits in front of and behind the sample, two step motors for moving arms on which the source and detector was mounted, and an adjustable sample holder placed in the optical centre of the diffractometer, completed the set up. The complete experimental scattering parameter range, q = 0.05-17.00 Å^{-1} was explored by performing several measurements in correspondence with a set of scattering angles θ at 24.0°, 15.5°, 8.0°, 5.0°, 3.0°, 2.0°, 1.5° 1.0°, 0.5° and using the relation:

$$q = \frac{4\pi \sin \vartheta}{\lambda} = EC \sin \vartheta \qquad (1)$$

where q is expressed in [Å^{-1}], λ in [Å]; the utilized energy range is E_{min}= 13.5 keV and E_{max}= 38.2 keV, and the value of the constant C

ADVANCED MATERIALS

is 1.014[(keV Å)$^{-1}$]. The experimental data were corrected for the following effects: escape peaks suppression, normalization to the incident radiation intensity, division by X-ray absorption and polarization coefficients, subtraction of the contributions, due to inelastic scattering, from the observed intensities $I(E,\theta)$ [44,45]. Then the spectra were joined to reconstruct the whole diffraction pattern. The complete function covers a wide range in the reciprocal space from 0.05 to 17.0 Å^{-1}. Atomic scattering factors, $f_h(q)$, were taken from International Tables [46]. The experimental static structure function was calculated as

$$i(q) = I_{coh}(E,\vartheta) - \sum\nolimits_h f_h^2(q) \tag{2}$$

The experimental radial distribution $D(r)$ was obtained as

$$D(r) = 4\pi r^2\rho_0 + \frac{2r}{\pi}\int_0^{q_{max}} qi(q)M(q)\sin(qr)dq \tag{3}$$

where q indicates the scattering parameter, ρ_0 is the average electronic density of the sample $\left(\rho_0 = \left(\sum_h n_h f_h^2(0)\right) V{-}1\right)$, V is the stoichiometric unit volume chosen and $M(q)$ a modification function defined as: $M(q) = (f_S^2(0)/f_S^2(q))\exp(-0.01q^2)$. The experimental structure function and the experimental radial distribution function, in the form $D_{iff}(r) = D(r) - 4\pi\, r^2\rho_0$, are shown in Figure 1 and 2 respectively. Theoretical peak shapes were calculated by Fourier transforming the theoretical structure function, calculated by the Debye equation for the pair interactions of the theoretical models proposed:

$$i_{mn}(q) = \sum_{m\neq n}^{N} f_m(q)f_n(q)\frac{\sin(r_{mn}q)}{r_{mn}q}\exp(-\frac{1}{2}\sigma_{mn}^2q^2) \tag{4}$$

where r_{mn} corresponds to the distance between m and n atoms and σ_{mn} is the root-mean-square (r.m.s.) in the interatomic distance. The number of parameters was reduced by taking the same σ value for distances falling within predefined ranges r_{mn} , instead of using a different σ_{mn} value for each distance. The distance ranges of the interatomic interactions and the associated r.m.s. σ were determined and the values are reported in Table 3S. For calculating the best agreement between experimental data and theoretical peaks, we used the formula

$$R_{Hamilton} = \sqrt{\frac{\sum_{i=1}^{m}||F^e(q_i)| - |F^c(q_i)||^2}{\sum_{i=1}^{m}|F^c(q_i)|^2}} \tag{5}$$

where the i^{th} index runs over the m experimental points and the e and c labels of $F(q_i)$ refer to the experimental and calculated structural functions.

Received: September 8, 2006
Revised: October 20, 2006
Published online: October 26, 2007

[1] R. A. van Delden, T. Mecca, C. Rosini, B. L. Feringa, *Chem. Eur. J.* **2004**, *10*, 61.
[2] M. S. Taylor, E. N. Jacobsen, *Angew. Chem. Int. Ed.* **2006**, *45*, 1520.
[3] J. J. D. de Jong, L. N. Lucas, R. M. Kellogg, J. H. van Esch, B. L. Feringa, *Science* **2004**, *304*, 278.
[4] E. Yashima, K. Maeda, Y. Okamoto, *Nature* **1999**, *399*, 449.
[5] *The Porphyrin Handbook* (Eds: J. H. Chou, M. E. Kosal, H. S. Nalwa, N. A. Rakow, K. S. Suslick), Academic Press, New York, **2000**.
[6] J. M. Lehn, *Science* **2002**, *295*, 2400.
[7] A. Tanaka, K. Inoue, I. Hisaki, N. Tohnai, M. Miyata, A. Matsumoto, *Angew. Chem. Int. Ed.* **2006**, *45*, 4142.
[8] J. A. A. W. Elemans, A. E. Rowan, R. J. M. Nolte, *J. Mater. Chem.* **2003**, *13*, 2661.
[9] L. J. Prins, J. Huskens, F. de Jong, P. Timmermann, D. N. Reinhoudt, *Nature* **1999**, *398*, 498.
[10] J. M. Ribó, J. Crusats, F. Sagués, J. Claret, R. Rubires, *Science* **2001**, *292*, 2063.
[11] T. Yamaguchi, T. Kimura, H. Matsuda, T. Aida, *Angew. Chem. Int. Ed.* **2004**, *43*, 6350.
[12] H. Onouchi, T. Miyagawa, K. Morino, E. Yashima, *Angew. Chem. Int. Ed.* **2006**, *45*, 2381.
[13] R. Purrello, *Nat. Mater.* **2003**, *2*, 216.
[14] Y. Mizuno, T. Aida, K. Yamaguchi, *J. Am. Chem. Soc.* **2000**, *122*, 5278.
[15] J. Zhang, M. T. Albelda, Y. Liu, J. W. Canary, *Chirality* **2005**, *17*, 404.
[16] E. Bellacchio, R. Lauceri, S. Gurrieri, L. M. Scolaro, A. Romeo, R. Purrello, *J. Am. Chem. Soc.* **1998**, *120*, 12353.
[17] R. Lauceri, A. Raudino, L. M. Scolaro, N. Micali, R. Purrello, *J. Am. Chem. Soc.* **2002**, *124*, 894.
[18] R. Lauceri, R. Purrello, *Supramol. Chem.* **2005**, *17*, 61.
[19] A. Tsuda, E. Hirara, Y. S. Kim, H. Tanaka, T. Kawai, T. Aida, *Angew. Chem. Int. Ed.* **2004**, *43*, 6327.
[20] J. Crusats, J. Claret, I. Diez-Perez, Z. El-Hachemi, H. Garcia-Hortega, R. Rubires, F. Sagues, J. R. Ribò, *Chem.Commun.* **2003**, 1588.
[21] Y. Mizuno, Md. A. Alam, A. Tsuda, K. Kinbara, K. Yamaguchi, T. Aida, *Angew. Chem. Int. Ed.* **2006**, *45*, 3786.
[22] Y. Mizuno, T. Aida, *Chem.Commun.* **2003**, 20.
[23] K. Tashiro, K. Konishi, T. Aida, *J. Am. Chem. Soc.* **2000**, *122*, 7921.
[24] A. Mammana, M. De Napoli, L. Rosario, R. Purrello, *Bioorg. Med. Chem.* **2005**, *13*, 5419.
[25] R. Purrello, A. Raudino, L. M. Scolaro, A. Loisi, E. Bellacchio, R. Laceri, *J. Phys. Chem. B* **2000**, *104*, 10900.
[26] R. Purrello, L. M. Scolaro, E. Bellacchio, S. Gurrieri, A. Romeo, *Inorg. Chem.* **1998**, *37*, 3647.
[27] R. Caminiti, A. Capobianchi, P. Marovino, A. M. Paoletti, G. Padeletti, G. Pennesi, G. Rossi, *Thin Solid Films* **2001**, *382*, 70.
[28] *The Porphyrin Handbook* (Ed: M. O. Senge) Academic Press, Boston, **2000**.
[29] J. A Sheulnutt, X. Z. Song, J. G. Ma, S. L. Jia, W. Jentzen, C. J. Medforth, *Chem. Soc. Rev.* **1998**, *27*, 31.
[30] X. Z. Song, L. Jaquinod, W. Jentzen, D. J. Nurco, S. L. Jia, R. G. Khoury, J. G. Ma, C. J. Medforth, K. M. Smith, J. A. Sheulnutt, *Inorg. Chem.* **1998**, *37*, 2117.
[31] E. B. Fleischer, C. K. Miller, L. E. Webb, *J. Am. Chem. Soc.* **1964**, *86*, 2342.
[32] S. Geremia, L. Di Costanzo, G. Nardin, L. Randaccio, R. Purrello, D. Sciotto, R. Laceri, F. Picchierri, *Inorg. Chem.* **2004**, *43*, 7579.
[33] W. R. Sheidt, *J. Am. Chem. Soc.* **1974**, *96*, 90.
[34] J. C. Gallucci, P. N. Swepston, J. A. Ibers, *Acta Crystallogr. B* **1982**, *38*, 2134.
[35] X. Z. Song, L. Jaquinod, W. Jentzen, D. J. Nurco, S. L. Jia, R. G. Khoury, J. G. Ma, C. J. Medforth, K. M. Smith, J. A. Sheulnutt, *Inorg. Chem.* **1998**, *37*, 2009.
[36] A. Rosa, G. Ricciardi, E. J. Baerends, *J. Phys. Chem. A,* **2006**, *110*, 5180.
[37] S. J. Silvers, A. Tulinsky, *J. Am. Chem. Soc.* **1967**, *89*, 3331.
[38] S. Y. Ma, *Chem.Phys. Lett.* **2000**, *332*, 603.

[39] R. Matassa, E. Cervone, C. Sadun, *J. Porphyrins Phtalocyanines* **2003**, *07*, 579.
[40] See Supporting Information.
[41] R. Caminiti, C. Sadun, V. Rossi Alberini, F. Colloco, R. Felici, *XXV Italian Congress on Physical Chemistry* Cagliari, Italy, **1991**.
[42] M. Carbone, R. Caminiti, C. Sadun, *Trends in Chemical Physics Research* **2004**, *11*, 75.
[43] R. Caminiti, C. Sadun, V. Rossi Alberini, F. Colloco, R. Felici, *Patent RM/93 01261484* June 23, **1993**.
[44] K. Nishikawa, T. Iijima, *Bull. Chem. Soc. Jpn.* **1984**, *57*, 1750.
[45] G. Fritsch, D. A. Keimel, *Mat. Sci. Eng A.* **1991**, *134*, 888.
[46] *International Tables for X-ray Crystallography,* Kynoch Press, Birmingham, England **1974**.

